Available online at www.sciencedirect.com
ScienceDirect
Trans. Nonferrous Met. Soc. China 24(2014) 1117−1124
Transactions of Nonferrous Metals Society of China
www.tnmsc.cn

Numerical simulation of flow regions in red mud separation thickener's feedwell by analysis of residence-time distribution

Tian ZHOU[1,2], Mao LI[1,2], Qiu-long LI[1,2], Bo LEI[1,2], Qian-zhou CHENN[1,2,3], Jie-min ZHOU[1,2]

1. School of Energy Science and Engineering, Central South University, Changsha 410083, China;
2. Hunan Key Laboratory of Energy Conservation in Process Industry, Central South University, Changsha 410083, China;
3. Department of Mechanical Engineering, Purdue University Calumet, Hammond 46323-2094, United States

Received 19 April 2013; accepted 20 October 2013

Abstract: The residence-time distribution (RTD) and the compartment model were applied to characterizing the flow regions in red mud separation thickener's feedwells. Combined with the experimental work, validated mathematical model as well as three-dimensional computational fluid dynamics (CFD) model was established to analyze the flow regions of feedwells on an industrial scale. The concept of RTD, although a well-known method for the characterization of mixing behavior in conventional mixers and reactors, is still a novel measure for the characterization of mixing in feedwells. Numerical simulation results show that the inlet feed rate and the aspect ratio of feedwells are the most critical parameters which affect the RTD of feedwell. Further simulation experiments were then carried out. Under the optimal operation conditions, the volume fraction of dead zone can reduce by10.8% and an increasement of mixing flow volume fraction by 6.5% is also observed. There is an optimum feed inlet rate depending on the feedwell design. The CFD model in conjunction with the RTD analysis then can be used as an effective tool in the design, evaluation and optimization of thickener feedwell in the red mud separation.
Key words: computational fluid dynamics; residence-time distribution; compartment model; feedwell

1 Introduction

Thickeners are key unit in the Bayer alumina refining processing operations and are used to separate insoluble solid, usually red mud from the liquid feed slurry under the action of gravity. Thickeners enable the treatment of vast volumes of dilute feed slurry that passes through a central feedwell, with the intention of dissipating the incoming stream kinetic energy and gently discharging stream into the tank [1]. A rake, usually mounted on central shaft, is installed at the bottom of the thickener. As a result, the solids would settle down to form the dense underflow while the clarified liquor is collected at the peripheral overflow. Synthetic flocculant is often added to enhance settling by creating large fast settling aggregates which will provide the potential for greater throughput and higher utilization efficiency of the thickener.

The flow in the thickener's feedwells is of critical importance to the performance of the thickener as a whole since it is here that most stream's kinetic energy dissipation, flocculant mixing and aggregation process occur [2]. As a result, a quantitative description for the process mentioned above is therefore required. Furthermore, the transportation of the insoluble solids from feed slurry to various points in the tank is also governed by the hydrodynamic and turbulent mixing within the feedwell. Unless the feedwell is properly designed, detrimental effects can occur and have negative influence on settling. However, the thickening process is poorly understood and predictive design of thickening devices is still primarily empirical. It was indicated that the previous studies in the area did not supply sufficient insights for practical thickener design and operational issues [3]. Presently, the availability of method for feedwell design is far inadequate to meet the demand.

Numerical simulations have already proved their potential in the investigation for thickening process. A

Foundation item: Project (50876116) supported by the National Natural Science Foundation of China
Corresponding author: Mao LI; Tel: +86-13055169363; E-mail: limao89@163.com
DOI: 10.1016/S1003-6326(14)63170-8

number of publications have applied CFD to studying the hydrodynamics within thickeners as well as other industrial settling devices [4−7]; however, they merely focused on no-mineral applications and feedwells were not taken into consideration. PELOQUIN et al [8] applied conventional CFD to a bauxite residue thickener to show the flow patterns on the feedwell, and a optimization flow and solid concentration inside feedwell were gained by installing a baffle ring in the feedwell. WHITE et al [1] established a single-phase, three-dimensional CFD model to calculate the fluid flow in the feedwells, and the *k*-epsilon turbulence model was proven to be adequate enough to simulate the turbulent flow of the feedwell by experimental validation. The flocculation absorption mechanisms were combined into CFD calculation by KAHANE et al [2]. Modification on a plant feedwell was then carried out based on the CFD modeling and higher throughput was achieved [9]. TRIGLAVCANIN [10] modeled a number of design options for maintaining turbulence and mixing time in low aspect ratio feedwells, including alternative concepts from the manufactures. CFD investigation on feedwells has obviously been done by many institutes and thickener manufactures, but rarely published in any details due to confidential issues [11]. The flocculation process requires suitable mixing of the flocculant solutions with the incoming slurry. Such behaviors have rarely been studied and optimized since mixing conditions may not be an issue in many large, over-sized feedwells. However, the trend of high rate of red mud thickening as well as environmental and capital restriction requires higher demands on thickening performance in terms of throughput, over and under flow properties.

In this study, an investigation focused on mixing behaviors of the thickener's feedwell was performed using both numerical and experimental approaches. Numerical analysis was carried out by simulating the turbulent flow inside feedwells. The concept of RTD was applied to quantifying the mixing behavior for the thickener feedwells combining hydraulic model experiment validation based on the similarity theory. Then, a series of experiments were then carried out and the optimal operation condition based on the very design of the conventional feedwell was presented.

2 Residence-time distribution model and parameters of RTD curve

Residence-time [12], also known as removal time is the average time that a particle spends in a particular system. Unlike in ideal reactor system, the residence time of the fluid elements in the feedwells is not equal, which makes RTD be used for the characterization of the mixing conditions. The RTD is usually obtained by injecting a tracer instantaneously (a pulse input) or at a constant rate (a step input) at the inlet of the feedwells. The RTD function $E(t)$ can be then established by measuring the tracer concentration at the feedwell outlet as a function of time. $E(t)$ gives how much time different fluid elements have spent in the feedwell. Generally, the pulse input method is used since it can avoid the numerical errors in differentiation which is inherent in step input method. The RTD function is given in Eq. (1), where $C(t)$ is the tracer concentration at the feedwell outlet as a function of time.

$$E(t)=\frac{C(t)}{\int_0^{\infty}C(t)\mathrm{d}t} \tag{1}$$

When the RTD function is obtained, some parameters that can give quantitative description on the flow pattern can be calculated based on the compartment model [13−15].

Actual mean residence time can be written as follows:

$$t_{\mathrm{m}}=\frac{\int_0^{2\tau}tE(t)\mathrm{d}t}{\int_0^{2\tau}E(t)\mathrm{d}t} \tag{2}$$

Theoretical mean residence time can be written as follows:

$$\tau=\frac{V}{Q} \tag{3}$$

Dead volume fraction can be written as follows:

$$\frac{V_{\mathrm{d}}}{V}=1-\frac{t_{\mathrm{m}}}{\tau} \tag{4}$$

Dispersed plug volume fraction can be written as follows:

$$\frac{V_{\mathrm{p}}}{V}=\frac{t_{\max}}{\tau} \tag{5}$$

Mixed volume fraction can be written as follows:

$$\frac{V_{\mathrm{m}}}{V}=1-\frac{V_{\mathrm{d}}}{V}-\frac{V_{\mathrm{p}}}{V} \tag{6}$$

where t_{m} is the mean residence time which presents the average time of the fluids elements spend in the feedwell; V and Q represent the total volume fraction of the feedwell and incoming slurry volumetric flow rate, respectively; $t_{\max}$ is the time to obtain the maximum $E(t)$.

When investigating the flow mixing performance of the feedwells for different sizes or boundary conditions, a normalized RTD function $E(\theta)$ is incorporated by Eqs. (7) and (8), where θ is the dimensionless time.

$$E(\theta)=\tau E(t) \tag{7}$$

$$\theta=\frac{t}{\tau} \tag{8}$$

3 Physical and mathematical models

3.1 Physical model

As illustrated in Fig. 1, the thickener is a cylindrical tank with a cone-shaped bottom. The diameter of the tank is 22 m while the height of the thickener is 18 m. The incoming slurry passes through the feed pipe on which a self-dilute tube is mounted and enters the feedwell. A baffle ring is installed beneath the feed pipe entry of the feedwell. After mixing with the flocculant in the feedwell, the slurry enters into the tank of the thickener under the action of gravity. The clear liquor is collected through the overflow pipe at the upper peripheral of the tank, while the dense flow with high solid concentration settled at the bottom of the tank is drawn out through underflow pipe.

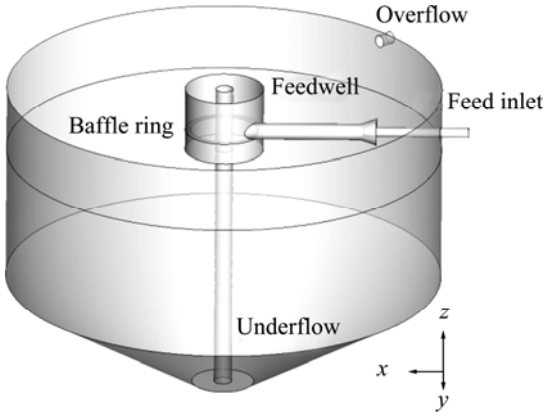

Fig. 1 Illustration of thickener model

3.2 Mathematical model

3.2.1 Governing equations

The mixture model, which is a simplified full Eulerian two-phase model with algebraic slip formulation of velocity, is used to model multiphase flow where the strong coupled phases move at different velocities, but local equilibrium is assumed over short spatial length scales. The steady three-dimensional, two-phase turbulent flow in feedwells is governed by the Navier−Stokes equations as [16]

$$\frac{\partial}{\partial t}(r_i\rho_i)+\nabla\cdot(r_i\rho_i\boldsymbol{U}_i)=0 \tag{9}$$

$$\frac{\partial}{\partial t}(r_i\rho_i\boldsymbol{U}_i)+\nabla\cdot(r_i\rho_i\boldsymbol{U}_i\boldsymbol{U}_j)= -r_i\nabla p+\nabla\cdot(\mu_{\text{eff}}r_i\nabla\boldsymbol{U}_i)+\boldsymbol{F}_i+r_i(\rho_i-\rho_l)\boldsymbol{g} \tag{10}$$

where $\boldsymbol{U}_i$, ρ_i and r_i are the velocity, density and volume fractions of phase i which can be either liquid or solid depending on its subscript; $\boldsymbol{F}_i$ is the drag force between the liquid and solid phases.

The drag function formulation can be prescribed following the Syamlal−O'Brien' work[16], which was based on measurements of the terminal velocities of particles in fluidized or settling beds.

$$f_{\text{drag}}=\frac{C_{\text{D}}Re_{\text{s}}\gamma_{\text{l}}}{24v_{\text{rs}}^2} \tag{11}$$

where γ_{l} represents the volume fraction of the fluid phase; C_{D} is the drag coefficient; Re_{s} is the relative Reynolds number; v_{rs} is the terminal velocity correlation for the solid phase.

3.2.2 Tracer

In order to obtain the RTD function, it is necessary to solve a transient species transportation equation of the tracer in the simulation.

$$\frac{\partial}{\partial t}(\rho Y_i)+\nabla\cdot(\rho\boldsymbol{U}Y_i)=-\nabla\cdot\boldsymbol{J}_i \tag{12}$$

where Y_i stands for the mass fraction of specie i, and $\boldsymbol{J}_i$ is the mass diffusion flux of specie i.

4 Boundary conditions and solution

The two-phase flow was considered in steady state and incompressible state. Transient calculations of the flow field and the solid particle tracer were carried out after the steady-state velocity field was obtained. There were one velocity inlet (feed pipe) and two velocity outlets (overflow and underflow) of the calculation domain. Non-slip conditions were applied for all the walls, and standard wall function was chosen. The upper surface of the tank as well as the feedwell was considered flat and was set to be symmetry.

The set of governing equations was solved with the help of the above boundary conditions numerically in a finite volume technique using the commercial CFD software Fluent. The thickener was assumed to contain the slurry initially and the calculation domain was initialized with the feed inlet velocity. The steady state calculation was converged until the solid concentration at the output became steady and the residual was below 0.001. Once the steady velocity field of the thickener was obtained, the transient calculation was carried out. The species transportation equation was solved by every time step along with continuity and momentum conservation equations, and the solution was converged within 20 iterations in each time step.

While solving the species transportation equation, the red mud particle tracer was injected through the inlet for 1 s, which was not supposed to affect the existing velocity field inside the thickener. The temporal value of the tracer concentration at the feedwell outlet was monitored to calculate the RTD curves of the feedwell.

5 Experimental

5.1 Apparatus

The apparatus of the hydraulic thickener model is shown in Fig. 2. The incoming flow rate of the fluid was controlled by a valve which has a flow meter installed for referencing. The hydraulic model was constructed at the geometry ratio of 1:20 compared with the thickener on an industrial scale.

The fluid flow in the feedwell was turbulent flow which was dominated by inertia force and gravity. As a result, the Froude number Fr was chosen as similarity number.

$$Fr = \frac{u_{\mathrm{p}}^2}{gl_{\mathrm{p}}} = \frac{u_{\mathrm{m}}^2}{gl_{\mathrm{m}}} \tag{13}$$

where subscript p stands for thickener prototype; m stands for hydraulic model; u is the fluid velocity; l presents the diameter of tracer particle; g is the gravitational acceleration.

Fig. 2 Photo of hydraulic thickener model for RTD experiment

5.2 Procedure

A finite number of particulate tracer method was used in order to quantitativly calculate the RTD curve of the feedwell. Pulverized coal was chosen as the tracer since they provided similar physical properties with the red mud agglomerates. 300 of pulverized coals were injected into the feed pipe to function as the tracer and the pulse input-response method was adopted in this work to determine RTD in the configuration studied due to its robustness. A high-speed camera system was parallelly located along with the feedwell's bottom plane to monitor tracer concentration data at the feedwell's output versus time. As shown in Fig. 3, a series of pictures that depict the time and quantity of coal particles leaving the feedwell were obtained and can be transformed to the tracer concentration at the output of the feedwell $C(t)$. Hence, the RTD curve and other evaluation parameters could be obtained through equations (1)−(8).

Replicate experiments were performed to establish high-repeatability data. Three different flow rates were studied with three replicates for each flow rate and the outcomes of these experimental runs show the desired repeatability of results.

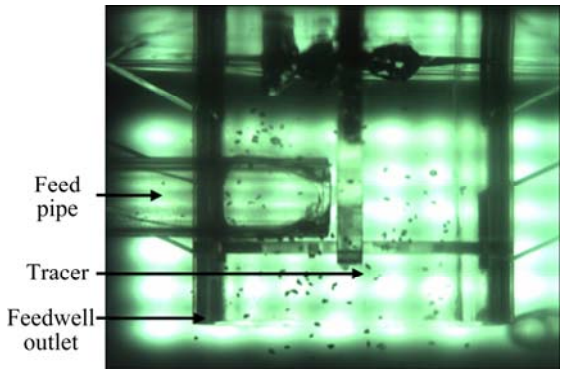

Fig. 3 Graphic example captured by high speed camera

6 Results and discussion

6.1 Validation

Numerical calculation was performed on the base case's thickener model with a feedwell aspect ratio of 1 and inlet flow rate of Q_{b}. The baffle ring position was fixed at z_{b} below the feed pipe in the z coordinate, as shown in Fig. 4.

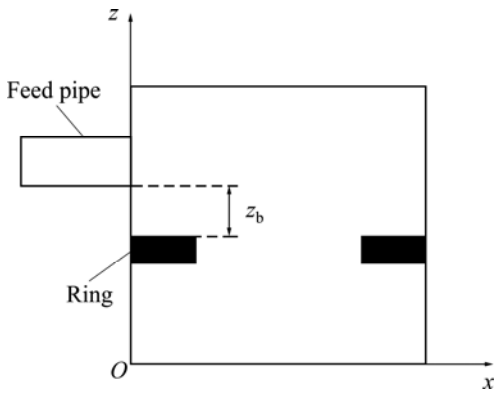

Fig. 4 Illustration of baffle position in feedwell

Meanwhile, the experiment was also carried out. The geometry similarity and Froude number were used to determine the boundary conditions for the experimental device. As shown in Fig. 5, the normalized RTD versus dimensionless time for experiment and the CFD simulation for the base case are in very good agreement. Table 1 shows that the RTD peak time of function of the $E(\theta)$ and volume fraction of dead zone for experiment and simulation are also in good agreement which both have the deviation less than 7%. This makes the validation of the numerical model in conjunction with the CFD code and then they can be used as a predictive tool in the design, evaluation and optimization of the flow in the feedwell.

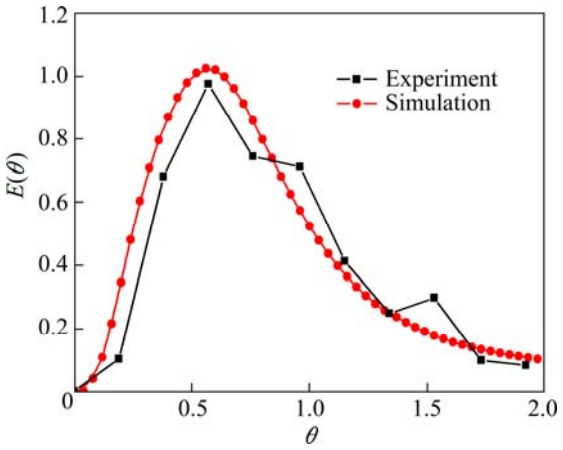

Fig. 5 RTD curves of CFD simulation and experiment

Table 1 RTD analysis result for CFD simulation and experiment

RTD analysis	t_{max}	(V_d/V)/%	Deviation/%
Experiment	0.56	25.36	1.7
Simulation	0.57	23.78	6.6

6.2 Parametric study

The CFD model enables the convenient study on the effect of changing some geometrical and operation parameters of the feedwell model. As a result, the following three parameters are selected since they are supposed to give the greatest impact on the mixing behavior of the feedwells [17], inlet slurry rate, aspect ratio of feedwell, and positions of the baffle ring. Six additional simulations were carried out by varying one parameter under reasonable industrial operation range at a time and fixing the other two values. All changed parameters were normalized to the base case and RTD curves were used for characterizing the mixing behavior for each case.

6.2.1 RTD curves under different inlet flow rates

The flow rate plays a principal role in determining the flow patterns in the feedwell, thereby another two simulations were performed with a increase to $1.2Q_b$ and a decrease to $0.8Q_b$ respectively based on the inlet flow rate of base case at Q_b.

The normalized RTD can be used as a analytical tool to evaluate the flow behavior in the feedwell. The flow pattern of the feedwell can be described as a combination of dispersed plug flow, mixing flow as well as a certain stagnant region. An obvious rising interval of the RTD curve represents the existence of the dispersed plug flow and the mixing zones. The long tails of the curves reveal that the stagnant zones exist. There is no obvious short-circuiting found in three curves since they give relative good smoothness.

Figure 6 provides the RTD curves of the feedwell of base case under different inlet feed rates and they illustrate a combination of plug-flow-mixing regime and a stagnant dead zone. There are obvious peaks on the curves, which are consistent with the existence of a plug flow and mixing region. However, some of the tracer leaves the feedwell before the theoretical mean residence time and there is a long tail since the tracer concentrations are still measured at two times the theoretical mean residence time. Hence, the stagnancy exists in terms of dead zones within the feedwell.

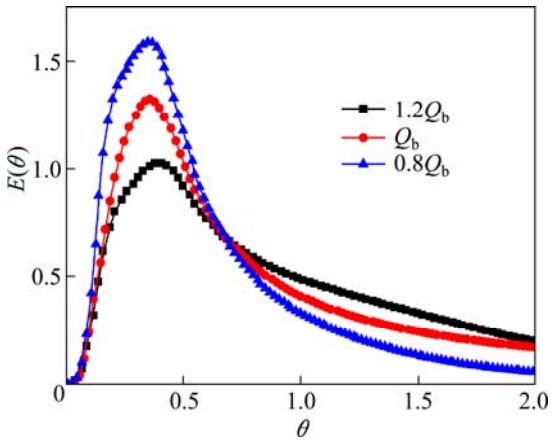

Fig. 6 RTD curves under different inlet flow rates

At a higher flow rate ($1.2Q_b$), the larger fraction of tracer tends to leave the feedwell at the time that is closer to the theoretical mean residence time (the point at θ=1.0 in the normalized time axis), suggesting that more volume is active in either plug flow or mixing zone. However, for a low inlet flow rate ($0.8Q_b$), large portion of the flow leaves the feedwell before the theoretical mean residence time due to large fraction of dead space.

Table 2 shows the evaluation parameters of RTD curves for three inlet flow rates. It is found that the stagnant volume decreases when the inlet flow rate increases. Furthermore, the increase of the mixing volume as well as the actual residence time with the increase of the inlet flow rate is observed. The case with the highest flow rate ($1.2Q_b$) gives the minimum volume fraction of 17.69% in dead zone, while the volume fraction of $0.8Q_b$ in dead zone is significantly increased to 34.77%. The actual residence time for the three cases shows nearly the same level and their theoretical residence time has an obvious difference from each other as well as the volume fraction of the plug flow. At fluid dynamic level, this is because higher flow rates may maintain the horizontal component of the swirling for longer time when feed enters the feedwell, and increase the residence time in the upper zone of the feedwell which ensures the efficiency of the feedwell. Therefore, better flocculation process is guaranteed since sufficient mixing region and adequate reaction time are provided. In contrast, a relative low flow rate leads to poor mixing

and insufficient horizontal component to swirling flow, which makes the upper region of the feedwell be not well utilized and may become the stagnant zone. Consequently, poor red mud agglomeration may occur and detrimental effect may also happen in the consequent separation settling.

Table 2 Parameters of RTD for different inlet flow rates

Flow rate	τ/s	t_{max}/s	t_m/s	(V_d/V)/%	(V_p/V)/%	(V_m/V)/%
$1.2Q_b$	41.20	17	33.91	17.69	41.26	41.04
Q_b	46.54	17	34.30	26.30	36.53	37.17
$0.8Q_b$	53.62	19	34.97	34.77	35.43	29.79

As a result, the higher flow rate ($1.2Q_b$) is more appropriate for our base case's feedwell since it provides the minimum dead volume fraction and the maximum mixing volume fraction with a reasonable residence time. On the other hand, the base case's feedwell is oversized designed for its designated flow rate due to its low operation efficiency.

6.2.2 RTD curves under different aspect ratios of feedwells

Flow patterns were calculated when alternating the aspect ratio of feedwells (the proportion for feedwell's diameter and height) upon different levels of 0.5, 1.0, 1.5 and the RTD curves are shown in Fig. 7. The appearance of the peak time tends to decrease as the aspect ratio of feedwell increases, which implies the reduction of the plug flow zone. On the other hand, the curves are shifted as the aspect ratio increases, suggesting that larger portion of the tracer leaves the feedwell before the theoretical mean residence time. Therefore, the inactive region of the feedwell is increased within the feedwell of larger diameter under the base condition's flow rate.

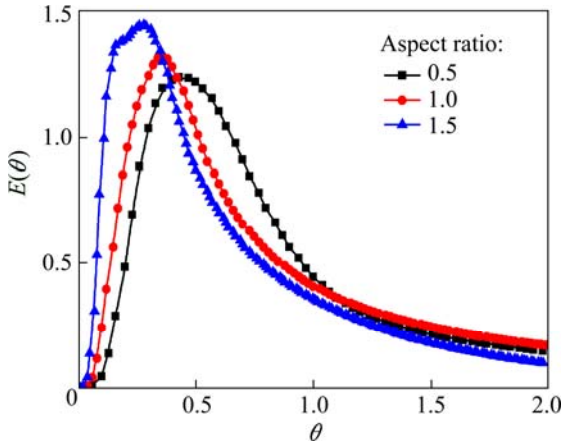

Fig. 7 RTD curves under different aspect ratios of feedwells

As shown in Table 3, when aspect ratio is decreased from 1.5 to 0.5, the dead zone fraction also decreases from 37.83% to 23.90% and the plug flow region increases dramatically from 28.21% to 43.68%. While the mixing areas do not show strong dependence on change of aspect ratio. When the radius reduces under a fixed flow rate, the swirling feed stream can be more deeply expanded to the stagnant zones of the feedwell in both radical and horizontal directions, implying an improvement on feedwell utilization efficiency. More uniform mixing for flocculant and red mud particles in the feedwell can be achieved, which will be a great help for consequent separation settling process. Furthermore, the plug flow areas increase with the reduction of the aspect ratio, which means that the dead zones shrink as they are mostly turned into active plug flow volume regions. The actual mean residence time decreases dramatically with the reduction of aspect ratio and the volume fraction for active regions is increased as the feedwell aspect ratio decreases. As a result, the base case presents a best operation condition among all the three feedwell aspect ratios since it provides a small dead zone and maximum fraction of mixing flow region. From the industrial application point of view, higher feedwell utilization is always wanted; however, the extent of the actual mean residence time of the feed and flocculant is of critical importance to the performance of the feedwell. This is because the flocculant requires a certain amount of time to capture the fine red mud particles and to form agglomerate. The required reaction time is, in general, still controlled empirically [18]. Hence, the consideration of the actual residence time of the feedwell should be taken according to the type of the flocculant during feedwell's design phase.

Table 3 Parameters of RTD for different aspect ratios

Aspect ratio	τ/s	t_{max}/s	t_m/s	(V_d/V)/%	(V_p/V)/%	(V_m/V)/%
1.5	70.88	20	44.06	37.83	28.21	33.94
1.0	46.54	17	34.30	26.30	36.53	37.17
0.5	29.75	13	22.64	23.90	43.68	32.40

6.2.3 RTD curves under different baffle ring positions of feedwells

As shown in Fig. 8, cases with three ring positions: $0.5z_b$, z_b, $2z_b$ were also simulated and the RTD curves are shown in Fig. 7. The different baffle rings positions merely changed the flow regions of the feedwell. However, the ring position at $0.5z_b$ gives a little better RTD curve shape since it has a relatively smaller dead zone area.

The parameters in Table 4 present the nearly identical flow region fractions for different ring positions. The ring position that is closer to the feed pipe; $0.5z_b$ has a little volume fraction of preferable dead zone as well as the actual residence time, which implies its

higher capability to hold the swirling motions of the feed stream.

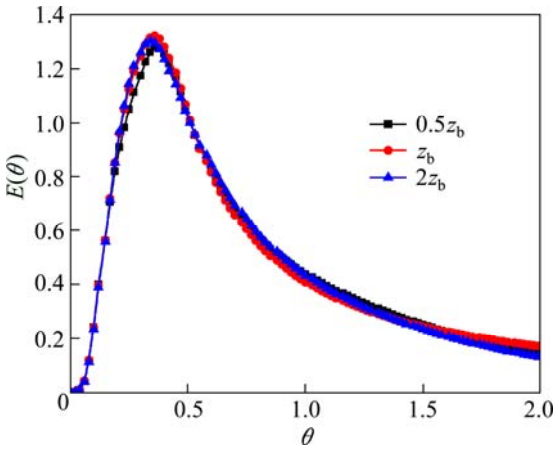

Fig. 8 RTD curves under different baffle ring positions

Table 4 Parameters of RTD for different ring positions

Ring position	τ/s	t_{max}/s	t_m/s	(V_d/V)/%	(V_p/V)/%	(V_m/V)/%
$2z_b$	46.54	16	33.80	27.37	34.38	38.25
z_b	46.54	17	34.30	26.30	36.53	37.17
$0.5z_b$	46.45	17	34.58	25.71	36.52	37.77

7 Optimization of parameters

The optimization experiment was then carried out to investigate the optimal parameters that influence the flow regions in the feedwell. Inlet flow rate and feedwell aspect ratio discussed in previous sections were chosen as the parameters with three levels for each. The levels are within reasonable industrial operation range based on the base case and the evaluation indexes for all the cases are shown in Table 5.

The experiment results indicated that with more specific change of the parameters, the flow regions in the feedwell show great difference from each other. From Table 5, it can be seen that case 2 has a minimum dead volume fraction of 15.26%, which provides the largest active flow region with the plug flow volume fraction of 41.26%, and 43.47% of its volume is occupied by mixing flow region. Compared with the base case, the optimal operation condition presented in case 2, can increase the volume fraction of mixing flow region by 6.5% and reduce the volume fraction of dead region by 10.8%.

Critical parameters, as which influence the flow behavior of the feedwell most, are the inlet feed rate and the aspect ratio of the feedwell. The inlet feed rates are process parameters which must be continuously controlled to obtain the expected performance of the feedwell. The aspect ratio of the feedwell is a design parameter that is set according to the operation target expected during the design of the equipment. Other parameters have marginal impact on the flow patterns of the feedwell.

Table 5 Parameters of RTD for parameter optimization

Experiment No.	τ/s	t_{max}/s	t_m/s	(V_d/V)/%	(V_p/V)/%	(V_m/V)/%
Base	46.54	17	34.30	26.30	36.52	37.17
1	26.18	14	20.35	23.50	53.46	23.05
2	41.20	17	34.91	15.26	41.26	43.47
3	61.56	13	41.74	32.19	21.17	46.68
4	29.75	13	22.04	25.92	43.58	30.39
5	70.88	20	44.06	37.83	28.15	33.95
6	34.97	18	27.74	20.69	51.47	29.83
7	53.62	19	34.97	34.77	35.43	29.78
8	78.55	13	48.63	38.09	16.54	45.35

8 Conclusions

1) A 3D thickener model was established and calculated to investigate the flow regions in a conventional feedwell under different flow rates, aspect ratios of feedwell as well as the baffle ring positions. The numerical model was validated through experimental results.

2) RTD curves and compartment model were used to quantify the flow region fractions in feedwells. The flow behavior in the feedwell can be described as a combination of dead zone, plug flow zone and mixing flow zone. Furthermore, the flow rate and aspect ratio of feedwell show a strong correlation with the constitution of different types of flow regions in the feedwell.

3) According to the simulation results, the inlet flow rate has a major influence on the transformation between the stagnant region and the mixing flow region while the aspect ratio of feedwell plays an important role in the transformation of the stagnant zone and plug flow volume. The position of the baffle ring has marginal impact on the flow regions of the feedwell.

4) The optimized condition can reduce the volume fraction of dead zone by 6.5% and increase the mixing region by 10.8%. There is an optimal range for inlet flow rate which is dependent on feedwell design. As a result, the CFD model and the RTD analysis methodology can be used as a predictive tool in the design, evaluation and optimization of the macro flow in the feedwell.

References

[1] WHITE R B, SUTALO I D, NGUYEN T. Fluid flow in thickener feedwell models [J]. Minerals Engineering, 2003, 16: 145−150.

[2] KAHANE R, NGUYEN T, SCHWARZ M P. CFD modelling of thickeners at Worsley Alumina Pty Ltd [J]. Applied Mathematical

Modelling, 2002, 26: 281−296.
[3] GLADMAN B J, USHER S P, SCALES P J. Understanding the thickening process [C]//2006 Australian Center for Geomechanics. Perth, Australia: Australia centre of Geomechanics, 2006: 5−12.
[4] WOOD M G, GREENFIELD P F, HOWES T, JOHNS M R, KELLER J. Computational fluid dynamics modelling of wastewater ponds to improve design [J]. Water Science and Technology, 1995, 31(12): 111−118.
[5] WEISS M, PLOSZ B G, ESSEMIANI K, MEINHOLD J. Suction-lift sludge removal and non-Newtonian flow behavior in circular secondary clarifiers: Numerical modelling and measurements [J]. Chemical Engineering Journal, 2007 132: 241−255.
[6] TEMLETOM M R, HOFMAN R, ANDREWS R C. Case study comparisons of computational fluid dynamics(CFD) modeling versus tracer testing for determining clearwell residence times in drinking water treatment [J]. Journal of Environmental Engineering and Science, 2006 5: 529−536.
[7] BEAK H K, PARK N S, KIM J H, LEE S J, SHIN H S. Examination of three-dimensional flow characteristics in the distribution channel to the flocculation basin using computational fluid dynamics simulation [J]. Journal of Water Supply: Research and Technology, 2005, 54(6): 349−354.
[8] PELOQUIN G, BUI R T, KOCAEFE D, SIMARD G. Mathematical modeling of red mud thickener [J]. The Canadian Journal of Chemical Engineering, 2005, 83: 458−465. (in French)
[9] KAHANE R B, SCHWARZ M P, JOHNSTON R R M. Residue thickener modeling at Worsley Alumina [J]. Applied Mathematical Modelling, 2002, 26: 281−296.
[10] TRIGLAVCANIN R A. The heart of thickener performance. [C]// 2008-Pcorceedings of the Eleventh International Seminar on Paste and Thickemer Tailings. Kasane, Botswana, 2009: 63−81.
[11] FAWELL P D, FARROW J B, HEATH A R, NGUYEN T V, OWEN A T, PATERSON D, RUDMAN M, SCALES P J, SIMIC K, STEPHENS D W, SWIFT D W, USHER S P. 20 years of AMIRA P266 “Improving thickener technology”: How has it changed the understanding of thickener performance? [C]//12th International Seminar on Paste and Thickened Tailings. Chile: Australian Centre for Geomechanics, 2009: 59−68.
[12] MACMULLIN R B, WEBER M. The theory of short-circuiting in continuous-flow mixing vessels in series and the kinetics of chemical reactions in such systems [J]. Chemical Engineering, 1935, 31: 409−458.
[13] MOUMTEZ B, AHMED B, KAMEL T. Numerical investigation of the fluid flow in continuous casting tundish using analysis of RTD curves [J]. Journal of Iron and Steel Research International, 2009, 16(2): 22−29.
[14] LEVENSPEIL O. Chemical reaction engineering [M]. 2nd ed. New York: Wiley and Sons, 1972: 257−320.
[15] JOHN T A, ADENIYI L. Numerical and experimental studies of mixing characteristics in a T-junction microchannel using residence time distribution [J]. Chemical Engineering Science, 2009, 64: 2234−2242.
[16] ZHOU Tian, LI Mao, CHENN Qian-zhou, ZHOU Jie-ming. Numerical simulation and optimization of the red mud separation thickener with self-dilute feed [J]. Journal of Central South University, 2014, 21(1): 344−350.
[17] SUTALO I D, PATERSON D A, RUDMAN M. Flow visualization and computational prediction in thickener rake models [J]. Minerals Engineering, 2003, 16: 93−102.
[18] ZHANG Yu-ming, LIU Gui-hua. The flocculant in red mud separation process [J]. Light Metals, 2002, 2: 10−14. (in Chinese)

赤泥分离沉降槽中心桶内停留时间分布的数值模拟

周 天[1,2]，李 茂[1,2]，李秋龙[1,2]，雷 波[1,2]，周 谦[1,2,3]，周孑民[1,2]

1. 中南大学 能源科学与工程学院，长沙 410083；
2. 中南大学 流程工业节能湖南省重点实验室，长沙 410083；
3. Department of Mechanical Engineering, Purdue University Calumet, Hammond 46323-2094, United States

摘 要：通过引入停留时间分布(RTD)和隔室模型，对赤泥分离沉降槽中心桶内流场流形开展数值模拟研究。结合实验结果，建立沉降槽中心桶的 3D 计算流体力学(CFD)模型。结果表明：在中心桶内存在复杂的流形，进料流量和中心桶的径高比对中心桶内流场流形有重要影响。通过进一步的优化实验，中心桶内死区的体积分数可减少 10.8%，混合区的体积分数可提升 6.5%。结合数值仿真模型计算和停留时间分布分析方法，该数值模拟可以应用于赤泥沉降槽中心桶的设计、评估以及优化。

关键词：计算流体动力学；停留时间分布；隔室模型；中心桶

(Edited by Xiang-qun LI)